arXiv:astro-ph/0408023v2 25 Aug 2004

Galaxy Assembly

By Eric F. Bell

Max-Planck-Institut für Astronomie, Königstuhl 17, D-69117 Heidelberg, Germany
bell@mpia.de

In a ΛCDM Universe, galaxies grow in mass both through star formation and through addition of already-formed stars in galaxy mergers. Because of this partial decoupling of these two modes of galaxy growth, I discuss each separately in this biased and incomplete review of galaxy assembly; first giving an overview of the cosmic-averaged star formation history, and then moving on to discuss the importance of major mergers in shaping the properties of present-day massive galaxies. The cosmic-averaged star formation rate, when integrated, is in reasonable agreement with the build-up of stellar mass density. Roughly 2/3 of all stellar mass is formed during an epoch of rapid star formation prior to $z \sim 1$, with the remaining 1/3 formed in the subsequent 9 Gyr during a period of rapidly-declining star formation rate. The epoch of important star formation in massive galaxies is essentially over. In contrast, a significant fraction of massive galaxies undergo a major merger at $z \lesssim 1$, as evidenced by close pair statistics, morphologically-disturbed galaxy counts, and the build-up of stellar mass in morphologically early-type galaxies. Each of these methods is highly uncertain; yet, taken together, it is not implausible that the massive galaxy population is strongly affected by late galaxy mergers, in excellent qualitative agreement with our understanding of galaxy evolution in a ΛCDM Universe.

1. Introduction

The last decade has witnessed amazing progress in our empirical and theoretical understanding of galaxy formation and evolution. This explosion in our understanding has been driven largely by technology: the profusion of 8–10-m class telescopes, the advent of wide-field multi-object spectrographs and imagers on large telescopes, servicing missions for the *Hubble Space Telescope* (HST), giving it higher resolution, higher sensitivity, larger field-of-view, and access to longer wavelengths, and the commissioning and/or launch of powerful observatories in the X-ray, ultraviolet, infrared, and sub-millimeter, are but a few of the important technological advances. This has led to a much-increased empirical understanding of broad phenomenologies: e.g., constraints on the overall shape of the cosmic history of star formation, the increased incidence of star-forming galaxies in less dense environments, the co-evolution of stellar bulges and the supermassive black holes that they host, and the increasing incidence of galaxy interactions at progressively higher redshifts, to name but a few. In turn, tension between these new observational constraints and models of galaxy formation and evolution have spurred on increasingly complex models, giving important (and sometimes predictive!) insight into the physical processes — star formation (SF), feedback, galaxy mergers, AGN activity — that are driving these phenomenologies.

In this review, I will give a grossly incomplete and biased overview of some hopefully interesting aspects of galaxy assembly. An important underpinning of this review is my (perhaps misguided) assumption that we live in a Universe whose broad properties are described reasonably well by the cold dark matter paradigm, with inclusion of a cosmological constant (ΛCDM): $\Omega_{\rm m} = 0.3$, $\Omega_\Lambda = 0.7$, and $H_0 = 70\,{\rm km\,s^{-1}\,Mpc^{-1}}$ following results from the *Wilkinson Microwave Anisotropy Probe* (Spergel et al. 2003) and the HST Key Project distance scale (Freedman et al. 2001). This model, while it has important and perplexing fine-tuning problems, seems to describe detection of 'cosmic jerk' using supernova type Ia (Riess et al. 2004), and the evolving clustering of the luminous

and dark matter content of the Universe with truly impressive accuracy on a wide range of spatial scales (Seljak et al. 2004).

An important feature of CDM models in general is that galaxies are formed 'bottom-up'; that is, small dark matter halos form first, and halo growth continues to the present through a combination of essentially smooth accretion and mergers of dark matter halos (e.g., Peebles 1980). Thus, small halos were formed very early, whereas larger haloes should still be growing through mergers. This has the important feature of decoupling, to a greater or lesser extent, the physics and timing of the formation of the stars in galaxies, and the assembly of the galaxies themselves from their progenitors through galaxy mergers and accretion (White & Rees 1978; White & Frenk 1991).

Accordingly, in this review I strive to explore the two issues separately. First, I will explore the build-up of the stellar mass in the Universe, irrespective of how it is split up into individual galaxies. Then, I will move on to describing some of the first efforts towards understanding how the galaxies themselves assembled into their present forms. This article will not touch on many important and interesting aspects of galaxy evolution; the co-evolution (or otherwise) of galaxy bulges and their supermassive black holes (see, e.g., Peterson, these proceedings; Ferrarese et al. 2001; Haehnelt 2004), the important influences of local environment on galaxy evolution (see, e.g., Bower & Balogh 2004), or the evolution of galaxy morphology (see, e.g., Franx, these proceedings). In this review, I adopt a ΛCDM cosmology and a Kroupa (2001) IMF; adoption of a Kennicutt (1983) IMF in this article would leave the results unchanged.

2. The assembly of stellar mass

In many ways, the empirical exploration of the assembly of stellar mass throughout cosmic history has been one of the defining features of the last decade of extragalactic astronomical effort. Yet, in spite of such effort, and the apparent simplicity of the goal, progress at times has been frustratingly slow. The difficulties are many: calibration of SF rate (SFR) and stellar mass indicators, the effects of dust on SFR estimates, relatively poor sensitivity for most SFR indicators, and field-to-field variations caused by large scale structure. In this section, I will briefly summarize the progress made to date towards measuring the cosmic SF history (SFH) using two independent methods: exploration of the evolution of the cosmic-averaged SFR, and the evolution of the cosmic-averaged stellar mass density, both as a function of epoch. The two are intimately related — the cosmic SFH is the integral over the cosmic SFR — and, barring any strong variation in stellar initial mass functions (IMFs) as a function of galaxy properties and/or epoch, consistency between the two would be expected.

2.1. *The cosmic-averaged star formation rate density*

2.1.1. *Methodology*

One measures SFR by measuring galaxy luminosities in a passband or passbands which one hopes will reflect the total number of massive stars in a galaxy. Using stellar population synthesis and other models, one then attempts to convert this luminosity into a total SFR, assuming a given stellar IMF to allow conversion from the number of massive stars to the total mass in the newly-formed stellar population (see, e.g., Kennicutt 1998 for an excellent review).

In some cases, this calibration from total luminosity to SFR is relatively robust, because it relies on reasonably well-understood physics. For example, the total ultraviolet (UV) light from a galaxy is reasonably robustly translated into the number of massive O and B stars. The total infrared luminosity of a starbursting galaxy, if the galaxy is

optically-thick to the UV light, is a reasonable reflection of the bolometric output of this starburst. Balmer line emission, under weak assumptions about the physical conditions in HII regions, is a reasonable indicator of the number of very massive O stars. These quantities, in turn, can be converted into a total SFR, assuming a stellar IMF which does not depend on galaxy properties and epoch.

In other cases, the calibration from luminosity to SFR is much less direct: e.g., the GHz radio emission from star-forming galaxies is well-correlated with other indicators of SFR, such as IR or Balmer line luminosity, and is known to be dominated by synchrotron emission from cosmic-ray electrons spiraling in galactic magnetic fields for at least massive star-forming galaxies (see Condon 1992 for an excellent review; see also Bell 2003). Yet, there is no robust theoretical understanding of why the relationship between radio emission and SFR should show such modest scatter (see, e.g., Bressan, Silva, & Granato 2002; Niklas & Beck 1997; Lisenfeld, Völk, & Xu 1996 for models of the radio emission of star-forming galaxies).

On top of these interpretive challenges, there are other important difficulties. Dust extinguishes UV light very effectively; empirical dust corrections based on UV color and/or UV-optical properties calibrated on UV-bright starbursts in the local Universe (Calzetti, Kinney, & Storchi-Bergmann 1994; Calzetti 2001) do not apply to normal galaxies (Bell 2002; Kong et al. 2004), IR-bright starbursts (Goldader et al. 2002), or indeed even HII regions (Bell et al. 2002; Gordon et al. 2004). Estimates of dust reddening from Balmer line ratios may yield reasonably accurate Balmer line-derived SFRs for galaxies (Kennicutt 1983), yet are extremely challenging to measure at $z \gtrsim 0.4$. IR and radio facilities lack the sensitivity to probe to faint limits; only galaxies with SFRs in excess of $\sim 10\,\mathrm{M}_\odot\,\mathrm{yr}^{-1}$ are observable with current facilities at $z \gtrsim 0.5$ (e.g., Flores et al. 1999).

2.1.2. *Results*

There are a huge number of papers which have addressed the evolution of the cosmic SFR, and are too numerous to mention or discuss in any detail. A few particularly important examples are Lilly et al. (1996), Madau et al. (1996), Flores et al. (1999), Steidel et al. (1999), and Haarsma et al. (2000).

In Fig. 1, I show the general form of the cosmic SFR, as derived by Hopkins (2004) in a very nice compilation of cosmic SFR estimates, where he uses locally-calibrated relationships between dust attenuation and SFR to correct for dust. His corrections are reasonably similar to those commonly used, but with the important advantages that they are uniformly derived, and account for the well-known SFR–dust correlation. The intention of showing this cosmic SFR is primarily to illustrate that despite the significant observational challenges and interpretive challenges it has been possible to determine its broad shape to better than a factor of three over much of cosmic history, using a variety of different observational methodologies.

There are two points which one should take away from the cosmic SFR, both of which have been known at least at the qualitative level since 1996 when the first cosmic SFRs were constructed (e.g., Lilly et al. 1996; Madau et al. 1996). Firstly, it is abundantly clear that the cosmic SFR has dropped by a factor of nearly 10 since $z \sim 1.5$ (see, e.g., the interesting compilation from Hogg 2001). Secondly, there is no compelling evidence against a roughly constant cosmic SFR at redshifts higher than 1 (e.g., Steidel et al. 1999), with the exception of some recent explorations of UV-derived SFRs at $z \gtrsim 4$, which appear to be lower than those at $z \lesssim 4$ (e.g., Stanway et al. 2004).

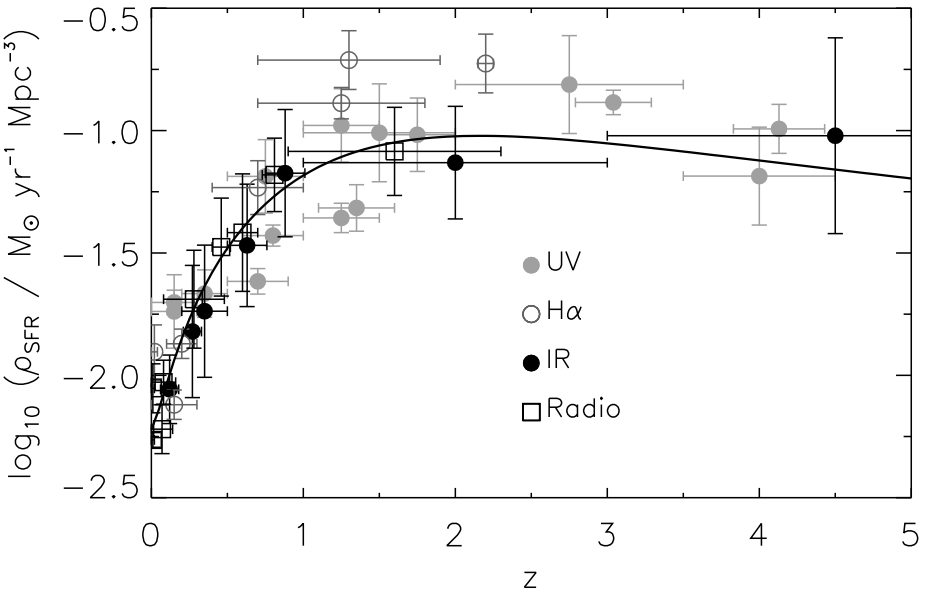


FIGURE 1. The evolution of the cosmic SFR density. SFRs assume a Kroupa (2001) IMF and $H_0 = 70\,\mathrm{km\,s^{-1}\,Mpc^{-1}}$. The data are taken from Hopkins (2004), and are corrected for dust assuming a SFR–dust correlation as found in the local Universe. The solid line shows an empirical fit to the cosmic SFR.

2.2. *The cosmic-averaged star formation history*

A complementary way to understand the star formation history of the Universe is to explore the build-up in stellar mass with cosmic time. This integral over the cosmic SFR contains the same information (under the assumption of a reasonably well-behaved stellar IMF), yet suffers from completely different systematic uncertainties and is therefore an invaluable probe of the broad evolution of the stellar content of the Universe.

2.2.1. *Methodology*

Ideally stellar masses would be estimated from spectroscopic data (e.g., velocity fields, rotation curves, and/or stellar velocity dispersions) coupled with multi-waveband photometry, under some set of assumptions about the dark matter content of the galaxy. Unfortunately, measurements of such quality are relatively uncommon, even in the local Universe.

In the absence of velocity data, one can attempt to estimate stellar masses using photometric data alone with the aid of stellar population synthesis models (e.g., Fioc & Rocca-Volmerange 1997; Bruzual & Charlot 2003). In these models, increasing the mean stellar age or the metallicity produces almost indistinguishable effects on their broad-band optical colors, and indeed even in their spectra with the exception of a few key absorption lines (e.g., Worthey 1994). Increasing dust extinction produces very similar effects at least some of the time (e.g., Tully et al. 1998), although the relationship between reddening and extinction is rather sensitive to star/dust geometry (Witt & Gordon 2000). An increase in stellar population age, metallicity or dust content reddens and dims the stellar population, at a fixed stellar mass. Crucially, the relationship between reddening

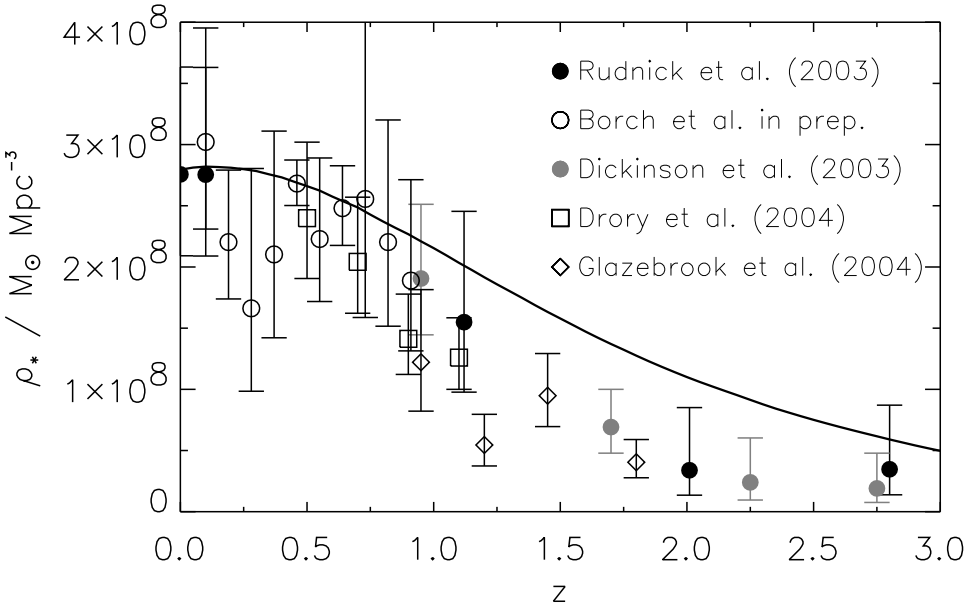


FIGURE 2. The evolution of the cosmic-averaged stellar mass density. Stellar masses assume a Kroupa (2001) IMF and $H_0 = 70\,\mathrm{km\,s^{-1}\,Mpc^{-1}}$. The data are taken from Rudnick et al. (2003; normalized to reproduce the $z = 0$ stellar mass density from Cole et al. 2001 & Bell et al. 2003), Dickinson et al. (2003), Drory et al. (2004), Glazebrook et al. (2004), and Borch et al.'s (in preparation) measurements from the COMBO-17 photometric redshift survey. The solid line shows the integral of the SFR from Fig. 1.

and dimming is similar for all three effects. While this makes it extremely challenging to measure the age, metallicity or dust content of galaxies using optical broad-band colors alone, it does mean that one can invert the argument and use color and luminosity to rather robustly estimate stellar mass, almost independent of galaxy SFH, metallicity or dust content (e.g., Bell & de Jong 2001).

The slope of the relationship between color and mass-to-light ratio (M/L) is passband-dependent (steeper in the blue, shallower in the near-infrared) but does not strongly depend on stellar IMF. In contrast, the zero point of the color–M/L relation depends strongly on stellar IMF, especially to its shape at masses $\lesssim 1M_\odot$ where the bulk of the stellar mass resides but the contribution to the total luminosity is low. There are important sources of systematic error: dust does not always move galaxies along the same color–M/L relation as defined by age and metallicity (e.g., Witt & Gordon 2000), and most importantly, significant contributions from young stellar populations (either because the galaxy is truly young or because of recent starburst activity) can bias the stellar M/Ls at a given color towards lower values. Recently, a number of methodologies have been developed to address these limitations by inclusion of important variations in star formation history (e.g., Papovich, Dickinson, & Ferguson 2001) or by using spectral indices and colors to account for bursts and dust more explicitly (e.g., Kauffmann et al. 2003).

2.2.2. *Results*

The basic methodology has been applied in the last several years to a wide variety of galaxy surveys to explore the stellar mass density in the local Universe (e.g., Cole et al. 2001; Bell et al. 2003), its evolution out to $z \sim 1$ (e.g., Brinchmann & Ellis 2000; Drory et al. 2004; Borch et al., in preparation) and even out to $z \sim 3$ (e.g., Rudnick et al. 2003; Dickinson et al. 2003; Fontana et al. 2003, Glazebrook et al. 2004). In Fig. 2, I show a compilation of some of these stellar mass estimates, all transformed to a Kroupa (2001) IMF. The error bars in all cases give a rough idea of the uncertainties in stellar mass; the error bars for Drory et al. (2004), Glazebrook et al. (2004), and Borch et al. include contributions from cosmic variance also.

From Figs. 1 and 2, it is clear that the epoch $z \gtrsim 1$ is characterized by rapid star formation, with roughly 2/3 of the stellar mass in the Universe being formed in the first 5 Gyr. In contrast, from $z \sim 1$ to the present day, one witnesses a striking decline in the cosmic SFR, by a factor of roughly 10. Despite this strongly suppressed SFR, roughly 1/3 of all stellar mass is formed in this interval, owing to the large amount of time between $z \sim 1$ and the present day.

2.3. *Are the cosmic star formation rates and histories consistent?*

It is interesting to test for consistency between the cosmic SFR and cosmic SFH — a lack of consistency between these two may give important insight into the form of the stellar IMF between $\sim 1 M_{\odot}$ (the mass range which optical/NIR light is most sensitive to) and $\gtrsim 5 M_{\odot}$ (the stellar mass range probed by SFR indicators), or the calibrations of or systematic errors in stellar mass and/or SFR determinations.

In order to integrate the cosmic SFR, I choose to roughly parameterize the form of the cosmic SFR following Cole et al. (2001). The cosmic SFR $\psi = (0.006 + 0.072 z^{1.35})/[1 + (z/2)^{2.4}] M_{\odot} \mathrm{yr}^{-1}\,\mathrm{Mpc}^{-3}$ provides a reasonable fit to the cosmic SFR (Fig. 1). The data are insufficient to constrain whether or not the cosmic SFR declines towards high redshifts from a maximum at $z \sim 1.5$; I choose to impose a mild decrease towards high redshift, primarily because that matches the evolution in integrated stellar mass slightly better than a flat evolution. This cosmic SFR is then integrated using the PEGASE stellar population model assuming a Kroupa (2001) IMF and an initial formation redshift $z_f = 5$. The exact integration in PEGASE accounts explicitly for the recycling of some of the initial stellar bass back into the interstellar medium; for the Kroupa (2001) IMF this fraction is $\sim 1/2$, i.e., stellar mass in long-lived stars is 1/2 of the stellar mass initially formed (for a Kennicutt 1983 IMF the fraction is similar). I show the expected cosmic SFH as the solid line in Fig. 2.

It is clear that the form of the cosmic SFR required in Fig. 1 reproduces rather well the cosmic SFH as presented in Fig. 2. There are some slight discrepancies; a cosmic SFR as flat as that shown in Fig. 1 appears to overpredict the amount of stellar mass that one sees at $z \sim 3$. This might indicate that a drop-off in cosmic SFR towards higher redshift is required, or may indicate that an IMF richer in high-mass stars is favored for high-redshift starbursts. Yet, it is important to remember that estimates of cosmic SFR and SFH are almost impossible to nail down with better than 30% accuracy at any redshift. At $z \gtrsim 1$ the constraints are substantially weaker still, owing to large uncertainties from large scale structure, uncertainties in the faint-end slope of the stellar mass or SFR functions used to extrapolate to total SFRs or masses, and the difficulty in measuring SFRs and masses of intensely star-forming, dusty galaxies. Therefore, I would tend to downweight this disagreement at $z \gtrsim 1.5$ until better and substantially deeper data are available, focusing instead on the rather pleasing overall agreement between these two independent probes of the cosmic SFH.

3. The assembly of galaxies

§2 focused on the broadest possible picture of the assembly of stellar mass — the build-up of the stellar population, averaged over cosmologically-significant volumes. Yet, the physical processes contributing to this evolution will be much more strongly probed by studying the demographics of the galaxy populations as they evolve. This splitting of the cosmic SFR/SFH can happen in many ways: study of the evolution of the luminosity function, stellar mass function, or SFR 'function', study of galaxies split by morphological type or rest-frame color, or by identification of galaxies during particular phases of their evolution (e.g., interactions). There has been a great deal of activity over the last decade towards this goal: implicit in the exploration of Figs. 1 and 2 is the construction of SFR and stellar mass functions, and a number of studies have explored the evolution of the galaxy population split by morphological type (e.g., Brinchmann & Ellis 2000, Im et al. 2002), rest-frame color (e.g., Lilly et al. 1996, Wolf et al. (2003), Bell et al. 2004b), or focusing on the role of galaxy interactions (e.g., Le Fèvre et al. 2000, Patton et al. 2002, Conselice et al. 2003).

A full and fair exploration of any or all of these goals is unfortunately beyond the scope of this work. Here, I choose to focus on one particular key issue: the importance of galaxy mergers in driving galaxy evolution in the epoch since $z \sim 3$, and especially at $z \lesssim 1$. Unlike the evolution of e.g., the stellar mass function or SFR function, to which both quiescent evolution and galaxy accretion can contribute, galaxy mergers (especially those at $z \lesssim 2$) are an unmistakable hallmark of the hierarchical assembly of galaxies. Therefore, exploration of galaxy mergers directly probes one of the key features of our current cosmological model.

I will focus here on exploring the number of major galaxy mergers (traditionally defined as those with mass ratios of 3:1 or less) over the last 10 Gyr. There are three complementary approaches to exploring merger rate, all of which suffer from important systematic uncertainties: the evolution of the fraction of galaxies in close pairs, the evolving fraction of galaxies with gross morphological irregularities, and investigation of the evolution of plausible merger remnants. In this work, I will briefly discuss all three methods, highlighting areas of particular uncertainty to encourage future development in this exciting and important field.

3.1. *The evolution of close galaxy pairs*

One of the most promising measures of galaxy merger rate is the evolution in the population of close galaxy pairs. Most close (often defined as being separated by $< 20\,\mathrm{kpc}$), bound galaxy pairs with roughly equal masses will merge within $\lesssim 1$ Gyr owing to strong dynamical friction (e.g., Patton et al. 2000). Thus, if it can be measured, the fraction of galaxies in physical close pairs is an excellent proxy for merger rate.

Accordingly, there have been a large number of studies which have attempted to measure close pair fraction evolution (a few examples are Zepf & Koo 1989, Carlberg, Pritchet, & Infante 1994, Le Fèvre et al. 2000; see Patton et al. 2000 for an extensive discussion of the background to this subject). In Fig. 3, I show the fraction of $M_B - 5\log_{10} h \lesssim -19.5$ galaxies in close $|\Delta_{\mathrm{proj}}| < 20h^{-1}\,\mathrm{kpc}$ pairs from Patton et al. (2000), Le Fèvre et al. (2000), and Patton et al. (2002). Patton et al. (2000) and Patton et al. (2002) explore the fraction of galaxies in close pairs with velocity differences $< 500\,\mathrm{kms}^{-1}$, whereas Le Fèvre et al. (2000) study projected galaxy pairs, and correct them for projection in a statistical way. Both studies, and indeed most other studies, paint a *broadly* consistent picture that the frequency of galaxy interactions was much higher in the past than at the present, and that the average $\sim L^*$ galaxy has suffered 0.1–1 major interaction between $z \sim 1$ and the present day. Small number statistics, coupled with differences

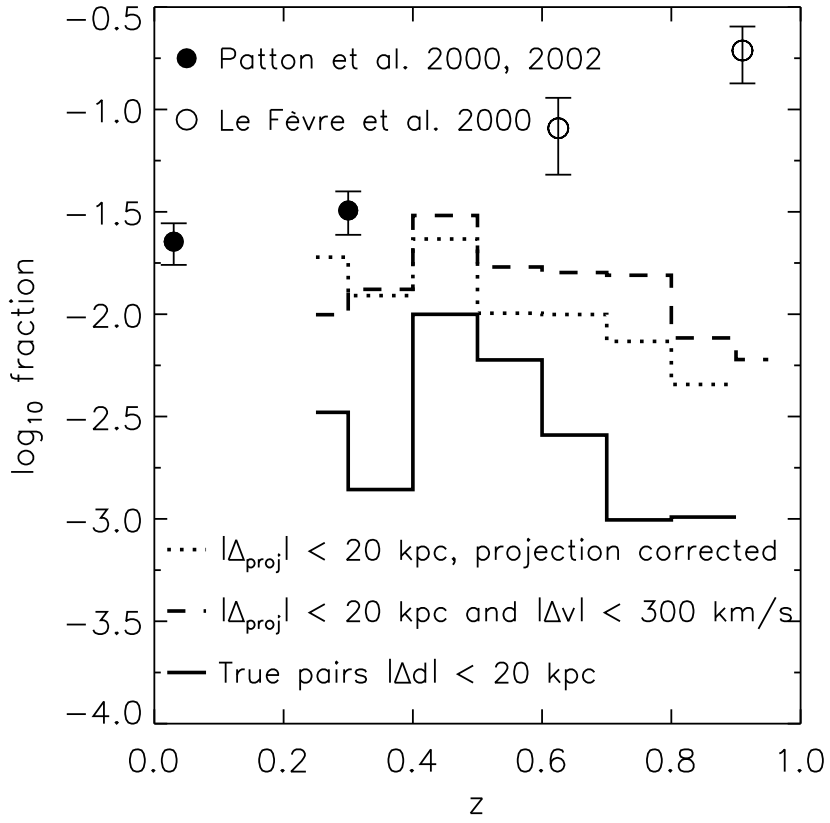


FIGURE 3. The evolution of the close pair fraction. Data points show measurements of the fraction of galaxies with 1 or more neighbors within a projected distance of $20h^{-1}$ kpc, corrected for projection (open points; Le Fèvre et al. 2000), and within a projected distance of $20h^{-1}$ kpc and a velocity separation of $< 500\,\mathrm{kms}^{-1}$ (solid points; Patton et al. 2000, 2002). The lines show the evolution of approximately equivalent measurements from the van Kampen et al. (in prep.) mock COMBO-17 catalogs: projection-corrected fraction (dotted line), the fraction of galaxies with $\geqslant 1$ neighbor within $20h^{-1}$ kpc and with velocity difference $< 300\,\mathrm{kms}^{-1}$ (dashed line), and the real fraction of galaxies with $\geqslant 1$ neighbor within $20h^{-1}$ kpc in real space.

in assumptions about how to transform pair fractions into merger rate, lead to a wide dispersion in the importance of major merging since $z \sim 1$.

Yet, there are significant obstacles to the interpretation of these, and indeed future, insights into galaxy major merger rate evolution. Technical issues, such as contamination from foreground or background galaxies, redshift incompleteness, and the construction of equivalent samples across the whole redshift range of interest must be thought about carefully (see, e.g., Patton et al. 2000, 2002). An further concern is that most close pair measurements are based on galaxies with similar magnitudes in the rest-frame optical. Bursts of tidally-triggered star formation may enhance the optical brightness of both galaxies in pairs, and the selection of galaxies with nearly equal optical brightness may not select a sample of galaxies with nearly equal stellar masses. Bundy et al.(2004) used K-band images of a sample of 190 galaxies with redshifts to explore this source of bias,

finding a substantially lower fraction of galaxies in nearly equal-mass close pairs than derived from optical data.

Yet, it is also vitally important to build one's intuition as to how the measured quantities relate to the true quantities of interest. As a crude example of this, I carry out the simple thought experiment where we compare the pair fraction derived from projection-corrected projected pair statistics (dotted line in Fig. 3), the pair fraction derived if one used spectroscopy to keep only those galaxies with $|\Delta v| < 300\,\mathrm{kms}^{-1}$ (dashed line), and the true fraction of galaxies with real space physical separation of $< 20h^{-1}\,\mathrm{kpc}$ (solid line). I use a mock COMBO-17 catalog under development by van Kampen et al. (in prep.; see Van Kampen, Jimenez, & Peacock 1999 for a description of this semi-numerical technique) to explore this issue; this model is used with their kind permission. It is important to note that this simulation is still under development; the match between the observations and models at $z \lesssim 0.5$ is mildly encouraging, although the generally flat evolution of pair fraction may not be a robust prediction of this model. Nonetheless, this model can be used to great effect to gain some insight into sources of bias and uncertainty.

The catalog is tailored to match the broad characteristics of the COMBO-17 survey to the largest extent possible (see Wolf et al. 2003 for a description of COMBO-17): it has $3 \times 1/4$ square degree fields, limited to $m_R < 24$ and with photometric redshift accuracy mimicking COMBO-17's as closely as possible. Primary galaxies with $m_R < 23$, $0.2 \leqslant z \leqslant 1.0$ and $M_V \leqslant -19$ are chosen; satellite galaxies are constrained only to have $m_R < 24$ and $|\Delta m_R| < 1\,\mathrm{mag}$ (i.e., to have a small luminosity difference). The dotted and dashed lines show the pair fraction recovered by approximately reproducing the methodologies of Le Fèvre et al. (2000; dotted line) and Patton et al. (2000, 2002; dashed line). It is clear that statistical field subtraction, adopted by Le Fèvre et al. (2000) and others, may be rather robust, in terms of recovering the trends that one sees with the spectroscopic+imaging data. The solid line shows the fraction of galaxies actually separated by $20h^{-1}\,\mathrm{kpc}$. It is clear that, at least in this simulation, many galaxies with projected close separation and small velocity difference are members of the primary galaxy's group which happen to lie close to the line of sight to the primary galaxy but are $\gtrsim 20$ kpc from the primary. In Le Fèvre et al. (2000), Patton et al. (2002), and other studies, this was often corrected for by multiplying the observed fraction by $0.5(1+z)$ following the analysis of Yee & Ellingson (1995); the data showed in Fig. 3 was corrected in this way. Our analysis of these preliminary COMBO-17 mock catalogs suggest that these corrections are uncertain, and that our current understanding of galaxy merger rate from close pairs may be biased. It is important to remember that the simulations discussed here are preliminary; the relationship between 'observed' and true close pair fractions may well be different from the trends predicted by the model. Yet, it is nonetheless clear that further modeling work is required before one can state with confidence that one understands the implications of close pair measurements.

3.2. *The evolution of morphologically-disturbed galaxies*

With the advent of relatively wide-area, high spatial resolution and S/N imaging from HST, it has become feasible to search for galaxy interactions by identifying morphologically-disturbed galaxies. There are a number of ways in which one can evaluate morphological disturbance: a few examples are by visual inspection (e.g., Arp 1966), residual structures in unsharp-masked or model-subtracted images (e.g., Schweizer & Seitzer 1992), automated measures of galaxy asymmetry (e.g., Conselice, Bershady, & Jangren 2000), or by the distribution of pixel brightnesses and 2nd-order moment of the light distribution (e.g., Lotz, Primack, & Madau 2004).

The important hallmarks that these different methodologies probe are the non-equilibrium

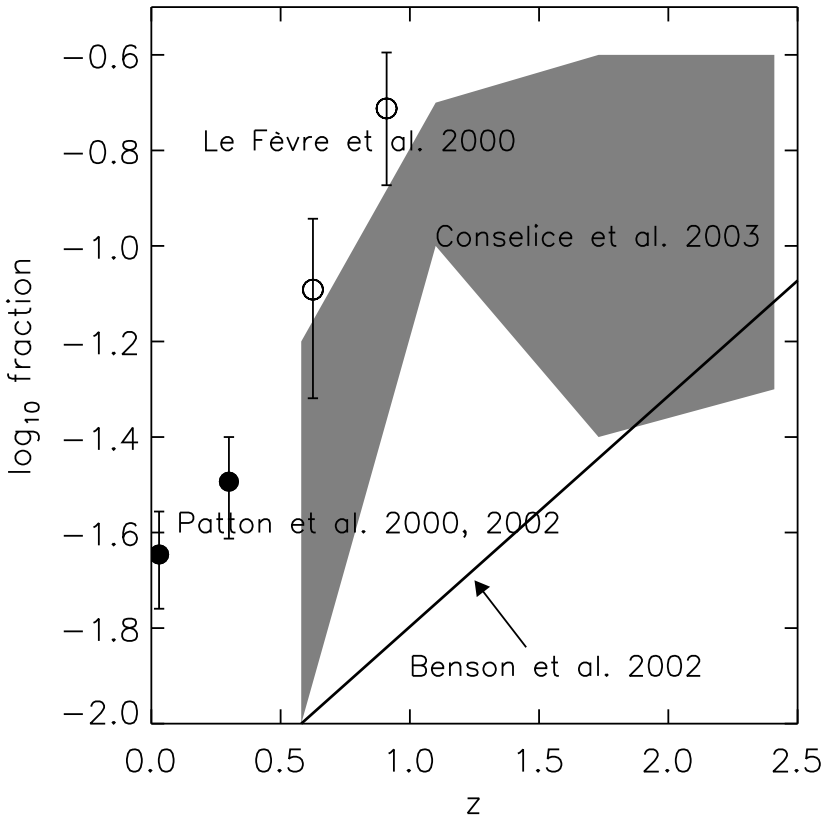


FIGURE 4. The evolution of merger rate as inferred from the fraction of galaxies with gross asymmetries (Conselice et al. 2003; grey shaded region). Inferred merger rates from close pairs are reproduced from Fig. 3 for comparison. A rough fit to predictions of major merger rate (visible for 1 Gyr) from the semi-analytic galaxy formation model of Benson et al. (2002), reproduced from Conselice et al. (2003), is shown by the solid line for reference.

signatures of tidal interaction — multiple nuclei and extended tidal tails. These features are common in simulations of interacting galaxies, and cannot result from quiescent secular evolution (e.g., Toomre & Toomre 1972, Barnes & Hernquist 1996). Visual inspection is a subjective way to pick out these structures, even to relatively low surface brightness limits; in contrast, automated measures of morphology typically quantify the amount of light in bright asymmetric structures, so pick out multiple bright patches or bright tidal tails rather effectively.

Recently, Conselice et al. (2003) have explored the fraction of galaxies with strong asymmetries in the rest-frame B-band our to redshift ~ 3 in the Hubble Deep Field North. Their results, for a similar absolute magnitude range as explored by Patton et al. (2002) and Le Fèvre et al. (2000), are shown in Fig. 4. While small number statistics (there are less than 500 galaxies contributing to the fractions), coupled with asymmetry uncertainties, are clearly an issue, a broadly consistent picture is painted whereby galaxy mergers were substantially more frequent at $z \gtrsim 1$, and have decreased in frequency until the present day. It is interesting to note that the observations are not well-reproduced by

the Benson et al. or van Kampen et al. models, which both predict substantially lower merger rates. Indeed, perhaps for the first time, observers are invoking the need for many more mergers than theorists!

While these first tentative steps are encouraging, there are a number of systematic uncertainties that should be considered carefully. At some level, contamination from projected close galaxy pairs is bound to be a problem. Samples of highly asymmetric galaxies will, correctly, include also some very close physically-associated galaxy pairs. Unfortunately, they will also contain a number of physically-unassociated close galaxy pairs: Le Fèvre et al. (2000) find that only $\sim 30\%$ of close galaxy pairs are likely to be physically-associated (in the sense of being in the same galaxy group; a smaller fraction still are genuine close pairs), and the mock COMBO-17 catalog analysis presented earlier suggests a fraction closer to 10%. These contaminants may be weeded out by source extraction software, as the pair of galaxy images may be parsed into 2 separate galaxies, each of which has a low asymmetry. Yet, if this image parsing is too enthusiastic, genuine major interactions may be parsed into multiple, individually rather symmetric, sub-units.

Furthermore, there are differences between different classification methodologies as to what constitutes a 'merger'. An example of this is given in Fig. 18 of Conselice et al. (2004), who explore the distribution of morphologically early-type galaxies (those with dominant bulge components), late-type galaxies (those with dominant disks), and peculiar galaxies (all other types, which includes merging and irregular galaxies) in the concentration (C) and asymmetry (A) plane. C is a measure of the light concentration of a galaxy profile, having high values for centrally-concentrated light profiles, and A is a measure of asymmetry, with high values denoting asymmetric galaxies. Inspecting their Fig. 18, one sees scattered trends between visual and automated classifications. Early-type galaxies tend to have higher concentrations and lower asymmetries, later types have lower concentrations and lower asymmetries, and peculiar systems have low concentrations and a wide range of asymmetries, with a tail to very high asymmetries. Yet, there are a number of early-types with low concentrations, and importantly a large number of peculiar galaxies have low asymmetries, and cannot be distinguished from morphologically-normal galaxies in this scheme. Preliminary comparisons between by-eye morphologies and C and A values for F606W images of galaxies in the GEMS (Galaxy Evolution from Morphology and SEDs; Rix et al. 2004) HST survey supports this conclusion, indicating that such automated schemes find it hard to differentiate between irregular galaxies (whose morphologies, to the human eye, indicate sporadic star formation triggered by internal processes) and clearly interacting galaxies with morphological features indicative of tidal interactions, such as multiple bright nuclei or tidal tails. A further complication is that the human eye is more sensitive to faint tidal tails in early- or late-stage mergers than automated schemes (i.e., the timescale probed by visual classifications may be longer than for automated schemes).

This discussion is by no means meant to detract from the value of the intriguing and ground-breaking work on merger rates from morphology; rather it is to emphasize that the measurement of merger rate is a subtle and difficult endeavor, fraught with systematic uncertainties which will likely have to be modeled explicitly using future generations of N-body, semi-analytic and SPH simulations, coupled with the artificial redshifting experiments already commonly used in this type of work.

3.3. *The evolution of plausible merger remnants*

From the earliest days of galaxy morphological classification, a population of galaxies whose light distribution is dominated by a smoothly distributed, spheroidal, centrally-concentrated light distribution was noticed. These *early-type galaxies* are largely sup-

ported by the random motions of their stars (Davies et al. 1983). These properties are very naturally interpreted as being the result of violent relaxation in a rapidly-changing potential well (Eggen, Lynden-Bell, & Sandage 1962). Therefore, in our present cosmological context, these galaxies are readily identified with the remnants of major galaxy mergers (e.g., Toomre & Toomre 1972; Barnes & Hernquist 1996). Detailed comparisons of simulated major merger remnants broadly supports this notion although some interesting discrepancies with observations remain, and are perhaps telling us about difficult-to-model gas-dynamical dissipative processes (e.g., Bendo & Barnes 2000; Meza et al. 2003; Naab & Brukert 2003). There is strong observational support for this notion — the correlation between fine morphological structure and residuals from the color–magnitude correlation (Schweizer & Seitzer 1992), the existence of kinematically-decoupled cores (e.g., Bender 1988), and the similarity between the stellar dynamical properties of late-stage IR-luminous galaxy mergers and elliptical galaxies (e.g., Genzel et al. 2001).

Therefore, study of the evolution of spheroid-dominated, early-type galaxies may be able to give important insight into the importance of galaxy merging through cosmic history. There are, as always, a variety of important complications and limitations to this approach. For example, a fraction of the galaxies becoming early-type during galaxy mergers will later re-accrete a gas disk, which will gradually transform into stars, making the galaxy into a later-type galaxy with a substantial bulge component (e.g., Baugh, Cole, & Frenk 1996). Furthermore, not all galaxy mergers will result in a spheroid-dominated galaxy; some lower mass-ratio interactions will result in a disk-dominated galaxy (e.g., Naab & Burkert 2003). In addition, it would be foolish to *a priori* ignore the possibility that an important fraction of early-type galaxies may be formed rapidly in mergers of very gas-rich progenitors at early epochs — a scenario reminiscent of the classical monolithic collapse picture (Larson 1974; Arimoto & Yoshii 1987). Yet, these interpretive complications, much as in all the cases discussed above, do not lessen the value of placing observational constraints on the phenomenology, with the confidence that our interpretation and understanding of the phenomenology will improve with time.

The rate of progress in this field has largely been determined by the availability of wide-format high-resolution imaging from HST. Ground-based resolution is insufficient to robustly distinguish disk-dominated and spheroid-dominated galaxies at cosmologically-interesting redshifts. In the local Universe, the vast majority of morphologically early-type galaxies occupy a relatively tight locus in color–magnitude space — the color–magnitude relation (e.g., Sandage & Visvanathan 1978; Bower, Lucey, & Ellis 1992; Schweizer & Seitzer 1992; Strateva et al. 2001). Therefore, many workers have focused on the evolution of the red galaxy population as an accessible alternative. The efficacy of this approach is only recently being tested. Accordingly, I explore the evolution of the red galaxy population first, turning subsequently to the evolution of the early-type population later.

3.3.1. *The evolution of the total stellar mass in red-sequence galaxies*

It has become apparent only in the last 5 years that the color distribution of galaxies is bimodal in both the local Universe (e.g., Strateva et al. 2001; Baldry et al. 2004) and out to $z \sim 1$ (Bell et al. 2004b). This permits a model-independent definition of red galaxies — those that lie on the color–magnitude relation. A slight complication is that the color of the red sequence evolves with time as the stars in red-sequence galaxies age, necessitating an evolving cut between the red sequence and the 'blue cloud'. The evolution of this cut means that some workers who explore the evolution of red galaxies using rather stringent color criteria — e.g., galaxies the color of local E/S0 galaxies

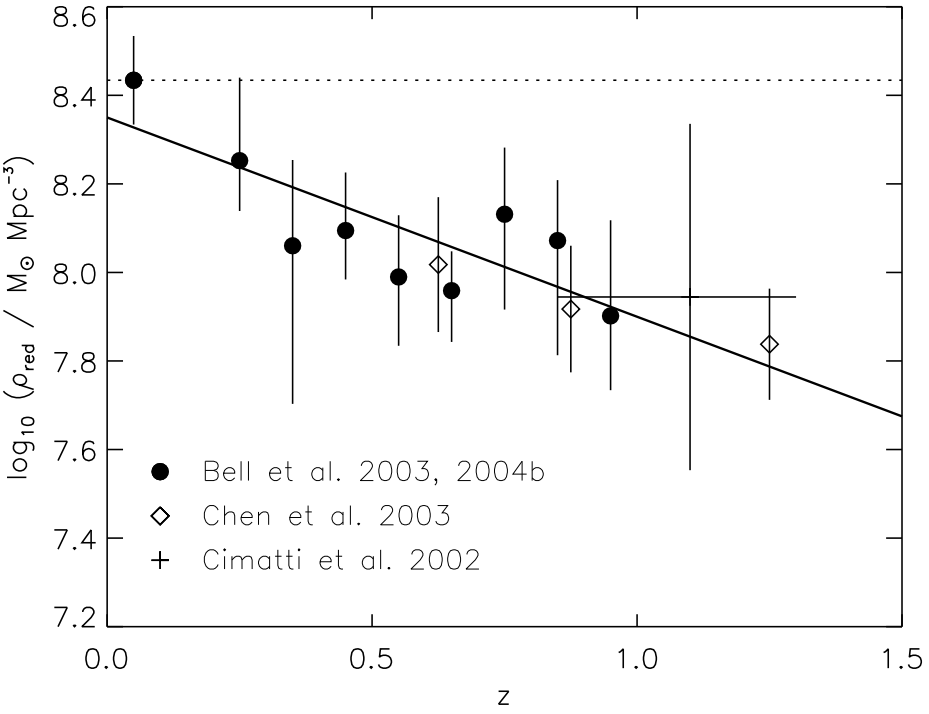


FIGURE 5. The evolution of the stellar mass density in red-sequence galaxies. Stellar masses assume a Kroupa (2001) IMF and $H_0 = 70\,\mathrm{km\,s^{-1}\,Mpc^{-1}}$. The local data point is taken from Bell (2003), and data for $0.2 < z < 1.3$ is taken from Bell et al. (2004b), Chen et al. (2003), and Cimatti et al. (2002). The solid line shows a rough fit to the total stellar mass density in red-sequence galaxies in the Cole et al. (2000) semi-analytic galaxy formation model. The dotted line shows the expected result if red-sequence galaxies were formed at $z \gg 1.5$ and simply aged to the present day.

— find much faster evolution in the red galaxy population than those who adopt less stringent or evolving cuts (e.g., Wolf et al. 2003).

Bearing this in mind, I show the evolution in the total stellar mass in red galaxies in Fig. 5. Although many surveys could in principle address this question (e.g., the surveys discussed in §2.2), very few have split their stellar mass evolution by color, and to date most surveys have only published evolution of luminosity densities in red galaxies. The $z = 0$ stellar mass density in red galaxies is from SDSS and 2MASS (Bell et al. 2003). The COMBO-17 datapoints for j_B evolution (Bell et al. 2004b) are converted to stellar mass using color-dependent stellar M/Ls as defined by Bell & de Jong (2001); extrapolation to total stellar mass density adopts a faint-end slope $\alpha = -0.6$, as found by Bell et al. (2003; 2004b) for red-sequence galaxies at $z \lesssim 1$. Error bars account for stellar mass uncertainties and cosmic variance, defined by the field-to-field scatter in stellar mass densities from the 3 COMBO-17 fields. Stellar masses for the LCIRS sample of red galaxies were estimated using the rest-frame R-band luminosity density presented by Chen et al. (2003), accounting for the mildest possible passive luminosity evolution (to account for evolution in stellar population color and luminosity in the most conservative way, so as to minimize any stellar mass evolution), and using a stellar

M/L for early-type galaxies from Bell & de Jong (2001) using a Kroupa (2001) IMF, and adopting a color of $B-R=1.5$ for early-type galaxies as a $z=0$ baseline. Error bars for include stellar mass estimation uncertainties and estimated cosmic variance, following Somerville et al. (2004). The K20 data point at $z\sim1.1$, derived from ERO 'old' galaxy space densities from Cimatti et al. (2002), is very roughly calculated using a number of doubtless poor assumptions. A (rather large) stellar mass of $\sim10^{11}M_{\odot}$ is attached to each galaxy, and the densities are multiplied by 2 to account for the star-forming EROs (the split was roughly 50:50). This stellar mass density was multiplied by 2 again to account for fainter, undetected galaxies. Error bars of ±0.2 dex and ±0.3 dex, combined in quadrature, account for cosmic variance following Somerville et al. (2004) plus our poor modeling assumptions. Owing to their use of discordant cosmologies, I do not show the inferred stellar mass evolution of the CFRS red galaxies in Fig. 5; however, like Bell et al. (2004b) they infer no evolution in the rest-frame B-band luminosity density to within their errors (Lilly et al. 1995), meaning that their stellar mass evolution would fall into excellent agreement with those of Bell et al. (2004b) or Chen et al. (2003).

The results are shown in Fig. 5. To first order, the luminosity density in the optical in red galaxies is constant out to $z\sim1$; this is confirmed by a number of surveys (e.g., Lilly et al. 1995, Chen et al. 2003, or Bell et al. 2004b). Coupled with the passive ageing of the stellar populations of these red galaxies (as is indicated by their steady reddening with cosmic time, and is confirmed by study of dynamically-derived M/Ls and absorption line ratios; e.g., Wuyts et al. 2004; Kelson et al. 2001), this implies a steadily increasing stellar mass density in red galaxies since $z\sim1.2$. *To date, to the best of our knowledge, there are no published determinations of red galaxy stellar mass or luminosity density which contradict this picture.*

The implications of this result are rather far-reaching. Bearing in mind that at $z\gtrsim1$ that the red galaxy population may be significantly contaminated and/or dominated by dusty star-forming galaxies (e.g., Yan & Thompson 2003, Moustakas et al. 2004), this evolution may well represent a strong upper limit to the stellar mass in early-type galaxies since $z\sim1.2$, unless large populations of very bright blue morphologically early-type galaxies are found. I address this question next, by exploring the stellar mass evolution in morphologically early-type galaxies since $z\sim1$.

3.3.2. *The evolution of the total stellar mass in early-type galaxies*

Owing to the lack of extensive wide-area HST-resolution imaging data, there are even weaker constraints on the evolution of stellar mass in morphologically early-type galaxies. We show published results from Im et al.(2002), Conselice et al. (2004), and Cross et al. (2004), supplementing them with a preliminary analysis of galaxies from GEMS and COMBO-17, which is presented with the permission of the GEMS and COMBO-17 teams.

Im et al.(2002) present a thorough study of the luminosity density evolution of E/S0 galaxies from the DEEP Groth Strip Survey, defined using bulge–disk decompositions and placing a limit on residual substructure in the model-subtracted images, supplemented with HST V and I-band imaging for 118 square arcminutes. A final sample of 145 E/S0 galaxies with $0.05<z<1.2$ are isolated. The fit of average early-type galaxy stellar M/L as a function of redshift from COMBO-17/GEMS; $\log_{10}\mathrm{M/L}_B=0.34-0.27z$, was used to transform the published B-band luminosity densities into stellar mass densities for the purposes of Fig. 6†. Cross et al. (2004) present rest-frame B-band luminosity functions for visually classified E/S0 galaxies in 5 ACS fields: the B-band luminosity den-

† Again, a Kroupa (2001) IMF was used.

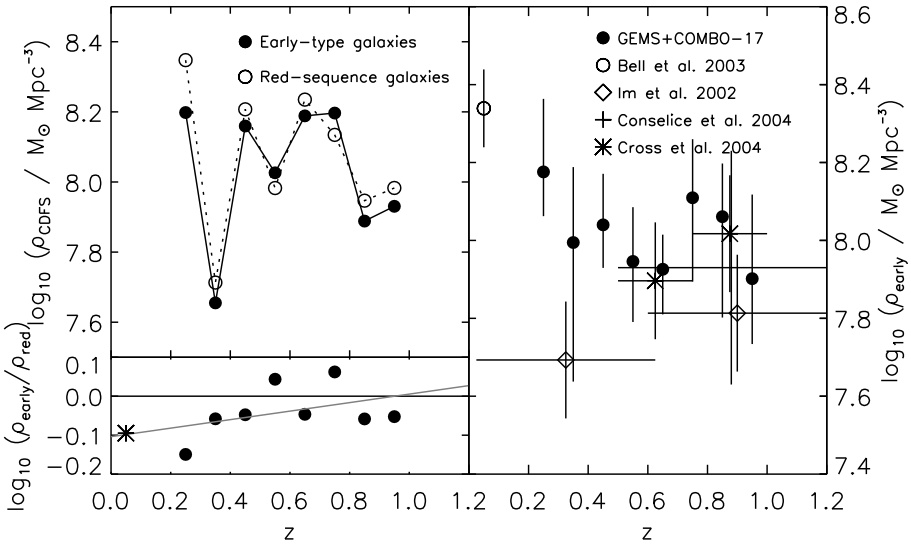


FIGURE 6. The evolution of the stellar mass density in early-type galaxies. Stellar masses assume a Kroupa (2001) IMF and $H_0 = 70\,\mathrm{km\,s^{-1}\,Mpc^{-1}}$. The left-hand panel shows the stellar mass densities from GEMS only; solid circles denote early-type galaxies and open circles red-sequence galaxies. The ratio of stellar mass in early-type galaxies to the red sequence is shown in the lower left panel; the asterisk is the local value taken from Bell (2003), and the grey line shows a linear fit to the GEMS data only (RMS $\sim$ 15%). The right-hand panel shows the resulting corrected early-type galaxy stellar mass density evolution, where again the local data are taken from Bell (2003), the solid circles denote the GEMS+COMBO-17 result, the diamonds show results from Im et al.(2002), the naked error bars show results from Conselice et al. (2004), and the asterisks show results from Cross et al. (2004).

sities were transformed into stellar mass in exactly the same way as for Im et al.(2002). Conselice et al. (2004) presented stellar mass densities directly, and these are reproduced on Fig. 6, after accounting for our use of a Kroupa (2001) IMF.

The preliminary GEMS/COMBO-17 early-type galaxy data points depict the evolution of total stellar mass in galaxies with Sérsic indices $n > 2.5$. In GEMS, Bell et al. (2004a) found that galaxies with $n > 2.5$ included $\sim$ 80% of the visually-classified E/S0/Sa galaxy population at $z \sim 0.7$, with $\sim$ 20% contamination from later galaxy types (recall, high Sérsic indices indicate concentrated light profiles). Here, in this very preliminary exploration of the issue, a $n = 2.5$ cut is adopted irrespective of redshift, ignoring the important issue of morphological k-correction. To recap, stellar masses are calculated using color-dependent stellar M/Ls from Bell & de Jong (2001), again extrapolating to total using a faint-end slope $\alpha = -0.6$.

The resulting $n > 2.5$ stellar mass evolution for the $30' \times 30'$ GEMS field is shown in the left panel of Fig. 6. One can clearly see strong variation in the stellar mass density of early-type galaxies, resulting from large scale structure along the line of sight. From such data, it is clearly not possible to place any but the most rudimentary and uninteresting limits on the evolution of early-type galaxies over the last 9 Gyr. Yet, noting that the bulk of early-type galaxies are in the red sequence at $z \sim 0$ (e.g., Strateva et al. 2001) and at $z \sim 0.7$ (e.g., Bell et al. 2004a), and that the stellar mass density of red-sequence galaxies undergo very similar fluctuations, it becomes interesting to ask if the ratio of stellar mass in red-sequence galaxies to early types varies more smoothly with redshift.

This is plotted in the lower left panel of Fig. 6. There is a weak trend in early-type galaxy to red-sequence galaxy mass density, caused by an increasingly important population of blue galaxies with $n > 2.5$ towards higher and higher redshift (see also Cross et al. 2004, who discuss this issue in much more depth). Importantly, however, there is only a $\sim 15\%$ scatter around this trend despite the nearly order of magnitude variation in galaxy density, arguing against strong environmental dependence in the early type to red galaxy ratio.

This relatively slow variation in early-type to red-sequence ratio (modeled using a simple linear fit for the purposes of this paper) is used to convert COMBO-17's stellar mass evolution in red galaxies from Fig. 5, which is much less sensitive to large scale structure, into the evolution of stellar mass density in morphologically early-type galaxies, which is shown in the right panel of Fig. 6. It is clear that there is a strongly increasing stellar mass density in morphologically early-type galaxies since $z \sim 1.2$†. While there are recent indications that lower-luminosity early-type galaxies are largely absent at $z \gtrsim 0.8$ (e.g., Kodama et al. 2004, de Lucia et al. 2004), the total stellar mass density is strongly dominated by $\sim L^*$ galaxies, and there is no room to avoid the conclusion that there has been a substantial build-up in the total number of $\sim L^*$ early-type galaxies since $z \sim 1.2$. Like the results presented in sections 3.1 and 3.2, these results suggest an important role for $z \lesssim 1$ galaxy mergers in shaping the present-day galaxy population‡.

3.4. *The importance of galaxy mergers since* $z \sim 1$

Three independent methods have been brought to bear on this problem — the evolution of close galaxy pairs, the evolution of morphologically-disturbed galaxies, and the evolution of early-type galaxies as a proxy for plausible merger remnants. All three methods suffer from important systematic and interpretive difficulties. Close galaxy pairs, even supplemented with spectroscopy to isolate galaxies within $\lesssim 500\,\mathrm{kms}^{-1}$ of each other, remain contaminated by galaxies in the same local structures. Some measures of morphological disturbance are susceptible to this source of error to a lesser extent, and a clear consensus on the meaning of the different automated and visual measures of morphological disturbance is yet to emerge. Early-type galaxies will be the result of only a subset of galaxy mergers and interactions, and the role of disk re-accretion and fading in driving early-type galaxy evolution is frustratingly unclear.

Yet, despite these difficulties some broad features are clear. Mergers between $\sim L^*$ galaxies are almost certainly more frequent at higher redshift than at the present day, but this does not imply by any means that galaxy mergers are unimportant at $z \sim 1$: indeed, it is possible that an average $\sim L^*$ galaxy undergoes roughly 1 merger between $z = 1$ and the present day (Le Fèvre et al. 2000). This is supported by the substantial build-up in stellar mass in red-sequence and early-type galaxies since $z \sim 1$. Substantial uncertainties remain and important questions, like the stellar mass dependence of the

† Im et al.(2002) report a low stellar mass density in early-type galaxies at $0.05 < z < 0.6$. We would attribute this deficiency in stellar mass to incompleteness at bright apparent magnitudes, leading to a deficit of nearby E/S0s with large stellar masses (as argued by Im et al. themselves), and perhaps to small number statistics and cosmic variance (as the volume probed by this study at $z \lesssim 0.5$ is rather small). Further work is required to explore further this discrepancy.

‡ Disk re-accretion and fading work in opposite directions in this context; disk accretion following a major merger takes galaxies away from the early-type class, whereas fading of disks which formed at earlier times will increase the relative prominence of spheroidal bulge components and add galaxies to the early-type class. A thorough investigation of these issues, involving bulge–disk decompositions of rest-frame B-band images of the GEMS sample and drawing on galaxy evolution models to build intuition of the importance and effects of different physical processes, is in preparation (Häußler et al., in prep.).

merger rate, or the fraction of dissipationless vs. dissipational mergers, are completely open. Nonetheless, these first, encouraging steps imply that the massive galaxy population is strongly affected by late galaxy mergers, in excellent qualitative agreement with our understanding of galaxy evolution in a ΛCDM Universe.

4. Summary and Outlook

The last decade has witnessed impressive progress in our understanding of galaxy formation and evolution. Despite important technical and interpretive difficulties, the broad phenomenology of galaxy assembly has been described with sufficient accuracy to start constraining models of galaxy formation and evolution. The history of star formation has attacked from two complementary and largely independent angles — through the evolution of the cosmic-averaged star formation rate, and through the build-up of stellar mass with cosmic time. Prior to $z \sim 1$, stars formed rapidly, and $\sim 2/3$ of the total present-day stellar mass was formed in this short ~ 4 Gyr interval. The epoch subsequent to $z \sim 1$ has seen a dramatic decline in cosmic-averaged SFR by a factor of roughly 10; however, $\sim 1/3$ of the present-day stellar mass was formed in this 9 Gyr interval. These two diagnostics of cosmic star formation history paint a largely consistent picture, giving confidence in its basic features.

The assembly of present-day galaxies from their progenitors through the process of galaxy mergers was studied using three largely independent diagnostics — the evolution of galaxy close pairs, the evolution of morphologically-disturbed galaxies, and the evolution of early-type galaxies as a plausible major merger remnant. The interpretive difficulties plaguing all three diagnostics are acute; accordingly our understanding of the importance of major mergers in shaping the present-day galaxy population is incomplete. Yet, all three diagnostics seem to indicate that an important fraction (dare I suggest $\gtrsim 1/2$?) of $\sim L^* \sim 3 \times 10^{10} M_\odot$ galaxies are affected by galaxy mergers since $z \sim 1$. This contrasts sharply with the form of the cosmic star formation history, where all of the action is essentially over by $z \sim 1$. It is not by any means indefensible to argue that late mergers shape the properties of the massive galaxy population in a way which is qualitatively consistent with our understanding of galaxy formation and evolution in a ΛCDM Universe.

Yet, it is clear that much work is to be done to fully characterize the physical processes driving galaxy evolution in the epoch since reionization $z \lesssim 6$. The 'shopping list' is too extensive to discuss properly, so I will focus on three aspects which I feel are particularly important.

4.1. *Our increasing understanding of the local Universe*

Wide area, uniform photometric and spectroscopic surveys, such as the Sloan Digital Sky Survey (SDSS; York et al. 2000), the Two Micron All Sky Survey (2MASS; Skrutskie et al. 1997), and the Two degree Field Galaxy Redsift Survey (2dFGRS; Colless et al. 2001) are revolutionizing our understanding of the local galaxy population. These surveys have allowed one to tie down the $z = 0$ data point for many evolutionary studies, greatly increasing the redshift and time-baseline leverage. Yet, this increased leverage is often difficult to fully apply, because local studies suffer from very different systematics than the lookback studies, and experimental details such as imaging depth, resolution, waveband, etc. are often imperfectly matched. At this stage, few groups have grasped the nettle of repackaging these local surveys in a format which can be readily artificially redshifted, etc. to allow for uniform analysis of the distant and local control samples. This will be an important feature of the most robust of the future works in galaxy evolution, and will

greatly increase the scope and discriminatory power of studies of galaxy photometric, dynamical, and morphological evolution.

4.2. *Using models as interpretive tools*

Large and uniform multi-wavelength and/or spectroscopic datasets are becoming increasingly common. An important consequence of this change in the nature of the data used to study galaxy evolution is that often the error budget is completely dominated by systematic and interpretive uncertainties. In this context, models of galaxy formation and evolution can help to understand and limit these systematic uncertainties through exhaustive analysis of realistic mock catalogs. A crude example of this kind of analysis is given in §3.1; a very nice example is the 2dFGRS group catalog of Eke et al. (2004). Mock simulations of this kind of quality must become a more prominent part of our toolkit in order for the kind of interpretive difficulties faced in §3.1 or §3.3 to be successfully navigated.

4.3. *The importance of multiple large HST fields*

Large scale structure is an important and frequently neglected source of systematic uncertainty (Somerville et al. 2004)†. Comparison of the left-hand and right-hand panels of Fig. 6 illustrates this point powerfully; the broad features of the evolution of early-type galaxy stellar mass density are discernable using the $30' \times 30'$ Chandra Deep Field South alone, but correction of this result for cosmic variance using the other two COMBO-17 fields yields a significantly more convincing picture. Yet, while this kind of correction for cosmic variance may work when there is significant overlap between populations of interest (although it is debatable how far one should push such an idea), it is not *a priori* clear that rarer and/or optically-obscured phases of galaxy evolution such as AGN or IR-luminous mergers will be well modelled with such techniques. Furthermore, short-timescale astronomical phenomena, such as AGN or galaxy mergers, have lower number density and are potentially very strongly clustered leading to large uncertainties from number statistics and cosmic variance. Yet, these phases of galaxy evolution, where galaxies undergo important and potentially permanent transformations in the cosmic blink of an eye, *require* HST-resolution data in order to explore their physical drivers.

When HST could be viewed as an essentially endless resource, a piecemeal approach was perfectly optimal: more and/or larger HST fields could be justified on a case-by-case basis, depending on the science goals of interest. Yet, faced with an unclear future for HST, it is not obvious that this approach is optimal. HST perhaps should be thought of as a fixed lifetime experiment, where the primary goal could become the creation of an archival dataset which will support 10–20 years of top-class research. In the creation of such an archival dataset, important questions will need to be addressed: availability of resources will need to be balanced against number statistics and cosmic variance, arguably at least 2 HST passbands will be required to allow some attempt at morphological k-correction, and deep multi-wavelength data will be required for study of black hole accretion and obscured star formation, naturally driving the fields into one of a small number of low HI and cirrus holes (see Papovich, these proceedings).

I wish to warmly thank the GEMS and COMBO-17 collaborations — Marco Barden, Steven Beckwith, Andrea Borch, John Caldwell, Simon Dye, Boris Häußler, Catherine Heymans, Knud Jahnke, Martina Kleinheinrich, Shardha Jogee, Daniel McIntosh, Klaus

† It is interesting to note that a $\times 10$ increase in area in a single contiguous field gives only a $\times 2$ reduction in cosmic variance, because the various parts of the single field are correlated with each other.

Meisenheimer, Chien Peng, Hans-Walter Rix, Sebastian Sanchez, Rachel Somerville, Lutz Wisotzki, and last but by no means least Christian Wolf — for their permission to present some GEMS and COMBO-17 results before their publication, for useful discussions, and for their friendship and collaboration. It is a joy to be part of these teams. I wish also to thank Eelco van Kampen and his collaborators for their efforts to construct mock COMBO-17 catalogs, for their permission to share results from these catalogs in this article, and for useful comments. Chris Conselice, Emmanuele Daddi, Sadegh Kochfar, and Casey Papovich are thanked for useful and thought-provoking discussions on some of the topics discussed in this review, and Chris Conselice and Shardha Jogee are thanked for constructive comments on the first version of this review. This work is supported by the European Community's Human Potential Program under contract HPRN-CT-2002-00316, SISCO.

REFERENCES

Arimoto, N., & Yoshii, Y. 1987 Chemical and photometric properties of a galactic wind model for elliptical galaxies A&A **173**, 23–38.

Arp, H. 1966 Atlas of Peculiar Galaxies *ApJS* **14**, 1–20.

Baldry, I. K., Glazebrook, K., Brinkmann, J., Ivezic, Z., Lupton, R. H., Nichol, R. C., & Szalay, A. S. 2004 Quantifying the Bimodal Color–Magnitude Distribution of Galaxies *ApJ* **600**, 681–694.

Barnes, J. E., Hernquist, L. 1996 Transformations of Galaxies II. Gasdynamics in Merging Disk Galaxies *ApJ* **471**, 115–142.

Baugh, C. M., Cole, S., & Frenk, C. S. 1996 Evolution of the Hubble sequence in hierarchical models for galaxy formation *MNRAS* **283**, 1361–1378.

Bell, E. F. 2002 Dust-induced Systematic Errors in Ultraviolet-derived Star Formation Rates *ApJ* **577**, 150–154.

Bell, E. F. 2003 Estimating Star Formation Rates from Far-infrared and Radio Luminosities: The Origin of the Radio–Far-infrared Correlation *ApJ* **586**, 794–813.

Bell, E. F., & de Jong, R. S. 2001 Stellar Mass-to-Light Ratios and the Tully–Fisher Relation *ApJ* **550**, 212–229.

Bell, E. F., Gordon, K. D., Kennicutt, Jr., R. C., & Zaritsky, D. 2002 The Effects of Dust in Simple Environments: Large Magellanic Cloud HII Regions *ApJ* **565**, 994–1010.

Bell, E. F., McIntosh, D. H., Katz, N., & Weinberg, M. D. 2003 The Optical and Near-IR Properties of Galaxies: I. Luminosity and Stellar Mass Functions *ApJS* **149**, 289–312.

Bell, E. F., et al. 2004a GEMS Imaging of Red Sequence Galaxies at $z \sim 0.7$: Dusty or Old? *ApJ* **600**, L11–14.

Bell, E. F., et al. 2004b Nearly 5000 Distant Early-Type Galaxies in COMBO-17: A Red Sequence and Its Evolution since $z \sim 1$ *ApJ* **608**, 752–767.

Bender, R. 1988 Rotating and counter-rotating cores in elliptical galaxies *A&A* **202**, L5–8.

Bendo, G. J., & Barnes, J. E. 2000 The line-of-sight velocity distributions of simulated merger remnants *MNRAS* **316**, 315–325.

Benson, A. J., Lacey, C. G., Baugh, C. M., Cole, S., & Frenk, C. S. 2002 The effects of photoionization on galaxy formation — I. Model and results at $z = 0$ *MNRAS* **333**, 156–176.

Bower, R. G., & Balogh, M. L. 2004 The Difference Between Clusters and Groups: A Journey from Cluster Cores to Their Outskirts and Beyond *Clusters of Galaxies: Probes of Cosmological Structure and Galaxy Evolution* (eds. J. S. Mulchaey, A. Dressler & A. Oemler), p. 326 Cambridge University Press

Bower, R. G., Lucey, J. R., & Ellis, R. S. 1992 Precision Photometry of Early Type Galaxies in the Coma and Virgo Clusters: a Test of the Universality of the Colour–magnitude Relation – II. Analysis *MNRAS* **254**, 601–603.

Brinchmann, J., & Ellis, R. S. 2000 The Mass Assembly and Star Formation Characteristics of Field Galaxies of Known Morphology *ApJ* **536**, L77–80.

Bressan, A., Silva, L., & Granato, G. L. 2002 Far infrared and radio emission in dusty starburst galaxies *A&A* **392**, 377–391.

Bruzual, G., & Charlot, S. 2003 Stellar population synthesis at the resolution of 2003 *MNRAS* **344**, 1000–1028.

Bundy, K., Fukugita, M., Ellis, R. S., Kodama, T., & Conselice, C. J. 2004 A Slow Merger History of Field Galaxies since $z \sim 1$ *ApJ* **601**, L123–126.

Calzetti, D. 2001 The Dust Opacity of Star-forming Galaxies *PASP* **113**, 1449–1485.

Calzetti, D., Kinney, A. L., & Storchi-Bergmann, T. 1994 Dust extinction of the stellar continua in starburst galaxies: The ultraviolet and optical extinction law *ApJ* **429**, 582–601.

Carlberg, R. G., Pritchet, C. J., & Infante, L. 1994 A survey of faint galaxy pairs *ApJ* **435**, 540–547.

Chen, H.-W., et al. 2003 The Las Campanas Infrared Survey IV. The Photometric Redshift Survey and the Rest-Frame R-Band Galaxy Luminosity Function at $0.5 \leqslant z \leqslant 1.5$ *ApJ* **586**, 745–764.

Cimatti, A., et al. 2002 The K20 survey – I. Disentangling old and dusty star-forming galaxies in the ERO population *A&A* **381**, L68–72.

Cole, S., Lacey, C. G., Baugh, C. M., Frenk, C. S. 2000 Hierarchical galaxy formation *MNRAS* **319**, 168–204.

Cole, S., et al. 2001 The 2dF galaxy redshift survey: near-infrared galaxy luminosity functions *MNRAS* **326**, 255-273.

Colless, M., et al. 2001 The 2dF Galaxy Redshift Survey: spectra and redshifts *MNRAS* **328**, 1039–1063.

Condon, J. J. 1992 Radio emission from normal galaxies *ARA&A* **30**, 575–611.

Conselice, C. J., Bershady, M. A., Jangren, A. 2000 The Asymmetry of Galaxies: Physical Morphology for Nearby and High-Redshift Galaxies *ApJ* **529**, 886–910.

Conselice, C. J., Bershady, M. A., Dickinson, M., & Papovich, C. 2003 A Direct Measurement of Major Galaxy Mergers at $z \lesssim 3$ *AJ* **126**, 1183–1207.

Conselice, C. J., Blackburne, J. A., & Papovich, C. 2004 The luminosity, stellar mass, and number density evolution of field galaxies of known morphology from $z = 0.5 - 3$ submitted to the *ApJ* (astro-ph/0405001).

Cross, N. J. C., et al. 2004 The luminosity function of early-type field galaxies at $z \sim 0.75$ *AJ*, in press (astro-ph/0407644).

Davies, R. L., Efstathiou, G., Fall, S. M., Illingworth, G., Schechter, P. L. 1983 The kinematic properties of faint elliptical galaxies *ApJ* **266**, 41–57.

de Lucia, G., et al. 2004 The Buildup of the Red Sequence in Galaxy Clusters since $z \sim 0.8$ *ApJ* **610**, L77–80.

Dickinson, M. E., Papovich, C., Ferguson, H. C., & Budavári, T. 2003 The Evolution of the Global Stellar Mass Density at $0 < z < 3$ *ApJ* **587**, 25–40.

Drory, N., Bender, R., Feulner, G., Hopp, U., Maraston, C. Snigula, J., & Hill, G. J. 2004 The Munich Near-Infrared Cluster Survey (MUNICS) VI. The Stellar Masses of K-Band-selected Field Galaxies to $z \sim 1.2$ *ApJ* **608**, 742–751.

Eggen, O. J., Lynden-Bell, D., Sandage, A. R. 1962 Evidence from the motions of old stars that the Galaxy collapsed *ApJ* **136**, 748–766.

Eke, V. R., et al. 2004 Galaxy groups in the 2dFGRS: the group-finding algorithm and the 2PIGG catalogue *MNRAS* **348**, 866–878.

Ferrarese, L., Pogge, R. W., Peterson, B. M., Merritt, D., Wandel, A., Joseph, C. L. 2001 Supermassive Black Holes in Active Galactic Nuclei – I. The Consistency of Black Hole Masses in Quiescent and Active Galaxies *ApJ* **555**, L79–82.

Fioc, M., & Rocca-Volmerange, B. 1997 PEGASE: a UV to NIR spectral evolution model of galaxies. Application to the calibration of bright galaxy counts. *A&A* **326**, 950–962.

Flores, H., et al. 1999 15μm ISO Observations of the 1415+52 CFRS Field: The Cosmic SFR as Derived from Deep UV, Optical, Mid-IR, and Radio Photometry *ApJ* **517**, 148–167.

Fontana, A., et al. 2003 The Assembly of Massive Galaxies from Near-Infrared Observations of the Hubble Deep Field South *ApJ* **594**, L9–12.

Freedman, W. L., et al. 2001 Final Results from the Hubble Space Telescope Key Project to Measure the Hubble Constant *ApJ* **553**, 47–72.

Genzel, R., Tacconi, L. J., Rigopoulou, D., Lutz, D., Tecza, M. 2001 Ultraluminous Infrared Mergers: Elliptical Galaxies in Formation? *ApJ* **563**, 527–545.

Glazebrook, K., et al. 2004 A high abundance of massive galaxies 3–6 billion years after the Big Bang *Nature* **430**, 181–184.

Goldader, J. D., et al. 2002 Far-Infrared Galaxies in the Far-Ultraviolet *ApJ* **568**, 651–678.

Gordon, K. D., et al. 2004 Spatially Resolved Ultraviolet, Hα, Infrared, and Radio Star Formation in M81 *ApJS* in press. (astro-ph/0406064)

Haarsma, D. B., Partridge, R. B., Windhorst, R. A., & Richards, E. A. 2000 Faint Radio Sources and Star Formation History *ApJ* **544**, 641–658.

Haehnelt, M. G. 2004 Joint Formation of Supermassive Black Holes and Galaxies. In *Coevolution of Black Holes and Galaxies* (ed. L. C. Ho), p. 406. Cambridge University Press.

Hogg, D. W. 2001 A meta-analysis of cosmic star-formation history *submitted to PASP* (astro-ph/0105280)

Hopkins, A. M. 2004 On the Evolution of Star Forming Galaxies *ApJ* in press. (astro-ph/0407170)

Im, M., et al. 2002 The DEEP Groth Strip Survey X. Number Density and Luminosity Function of Field E/S0 Galaxies at $z < 1$ *ApJ* **571**, 136–171.

Kauffmann, G., et al. 2003 Stellar masses and star formation histories for 10^5 galaxies from the Sloan Digital Sky Survey *MNRAS* **341**, 33–53.

Kelson, D. D., Illingworth, G. D., Franx, M., & van Dokkum, P. G. 2001 The Evolution of Balmer Absorption-Line Strengths in E/S0 Galaxies from $z = 0$ to $z = 0.83$ *ApJ* **522**, L17–21.

Kennicutt, Jr., R. C. 1983 The rate of star formation in normal disk galaxies *ApJ* **272**, 54–67.

Kennicutt, Jr., R. C. 1998 Star Formation in Galaxies Along the Hubble Sequence *ARA&A* **36**, 189–232.

Kodama, T., et al. 2004 Down-sizing in galaxy formation at $z \sim 1$ in the Subaru/XMM-Newton Deep Survey (SXDS) *MNRAS* **350**, 1005–1014.

Kong, X., Charlot, S., Brinchmann, J., Fall, S. M. 2004 Star formation history and dust content of galaxies drawn from ultraviolet surveys *MNRAS* **349**, 769–778.

Kroupa, P. 2001 On the variation of the initial mass function *MNRAS* **322**, 231–246.

Larson, R. B. 1974 Dynamical models for the formation and evolution of spherical galaxies *MNRAS* **166**, 585–616.

Le Fèvre, O., et al. 2000 Hubble Space Telescope imaging of the CFRS and LDSS redshift surveys – IV. Influence of mergers in the evolution of faint field galaxies from $z \sim 1$ *MNRAS* **311**, 565–575.

Lilly, S. J., Tresse, L., Hammer, F., Crampton, D., & Le Fèvre, O., 1995 The Canada-France Redshift Survey: VI. Evolution of the Galaxy Luminosity Function to $z \sim 1$ *ApJ* **455**, 108–124.

Lilly, S. J., Le Fèvre, O., Hammer, F., & Crampton, D. 1996 The Canada-France Redshift Survey: The Luminosity Density and Star Formation History of the Universe to $z \sim 1$ *ApJ* **460**, L1-4

Lisenfeld, U., Völk, H. J., & Xu, C. 1996 The FIR/radio correlation in starburst galaxies: constraints on starburst models *A&A* **314**, 745–753.

Lotz, J. M., Primack, J., & Madau, P. 2004 A New Nonparametric Approach to Galaxy Morphological Classification *AJ* **128**, 163–182.

Madau, P., Ferguson, H. C., Dickinson, M. E., Giavalisco, M., Steidel, C. C., & Fruchter, A. 1996 High-redshift galaxies in the Hubble Deep Field: colour selection and star formation history to $z \sim 4$ *MNRAS* **283**, 1388–1404.

Meza, A., Navarro, J. F., Steinmetz, M., & Eke, V. R. 2003 Simulations of Galaxy Formation in a ΛCDM Universe III. The Dissipative Formation of an Elliptical Galaxy *ApJ* **590**, 619–635.

Moustakas, L. A., et al. 2004 Morphologies and Spectral Energy Distributions of Extremely Red Galaxies in the GOODS-South Field *ApJ* **600**, L131–134.

Naab, T., & Burkert, A. 2003 Statistical Properties of Collisionless Equal- and Unequal-Mass Merger Remnants of Disk Galaxies *ApJ* **597**, 893–906.

Niklas, S., & Beck, R. 1997 A new approach to the radio–far infrared correlation for non-calorimeter galaxies *A&A* **320**, 54–64.

Papovich, C., Dickinson, M. E., & Ferguson, H. C. 2001 The Stellar Populations and Evolution of Lyman Break Galaxies *ApJ* **559**, 620–653.

Patton, D. R., et al. 2000 New Techniques for Relating Dynamically Close Galaxy Pairs to Merger and Accretion Rates: Application to the Second Southern Sky Redshift Survey *ApJ* **536**, 153–172.

Patton, D. R., et al. 2002 Dynamically Close Galaxy Pairs and Merger Rate Evolution in the CNOC2 Redshift Survey *ApJ* **565**, 208–222.

Peebles, P. J. E. 1980 *The large-scale structure of the universe*. Princeton, N. J.: Princeton University Press.

Riess, A. G., et al. 2004 Type Ia Supernova Discoveries at $z > 1$ from the Hubble Space Telescope: Evidence for Past Deceleration and Constraints on Dark Energy Evolution *ApJ* **607**, 665–687.

Rix, H.-W., et al. 2004 GEMS: Galaxy Evolution from Morphology and SEDs *ApJS* **152**, 163–173.

Rudnick, G., et al. 2003 The Rest-Frame Optical Luminosity Density, Color, and Stellar Mass Density of the Universe from $z = 0$ to $z = 3$ *ApJ* **599**, 847–864.

Sandage, A., & Visvanathan, N. 1978 The color-absolute magnitude relation for E and S0 galaxies. II – New colors, magnitudes, and types for 405 galaxies *ApJ* **223**, 707–729.

Schweizer, F., & Seitzer, P. 1992 Correlations between UBV colors and fine structure in E and S0 galaxies — A first attempt at dating ancient merger events *AJ* **104**, 1039–1067.

Seljak, U., et al. 2004 Cosmological parameter analysis including SDSS Ly-alpha forest and galaxy bias: constraints on the primordial spectrum of fluctuations, neutrino mass, and dark energy *submitted to PRD* (astro-ph/0407372).

Sérsic, J. L. 1968 *Atlas de Galaxias Australes*. Cordoba: Observatorio Astronomico.

Skrutskie, M. F., et al. 1997 The Two Micron All Sky Survey (2MASS): Overview and Status. in *The Impact of Large Scale Near-IR Sky Surveys* (eds. F. Garzon et al.) p. 25. Dordrecht: Kluwer Academic Publishing Company

Somerville, R. S., Lee, K., Ferguson, H. C., Gardner, J. P., Moustakas, L. A., & Giavalisco, M. 2004 Cosmic Variance in the Great Observatories Origins Deep Survey *ApJ* **600**, L171–174.

Spergel, D. N., et al. 2003 First-Year Wilkinson Microwave Anisotropy Probe (WMAP) Observations: Determination of Cosmological Parameters *ApJS* **148**, 175–194.

Stanway, E. R., Bunker, A. J., McMahon, R. G., Ellis, R. S., Treu, T., & McCarthy, P. J. 2004 Hubble Space Telescope Imaging and Keck Spectroscopy of $z \sim 6$ i-Band Dropout Galaxies in the Advanced Camera for Surveys GOODS Fields *ApJ* **607**, 704–720.

Steidel, C. C., Adelberger, K. L., Giavalisco, M., Dickinson, M., & Pettini, M. 1999 Lyman-Break Galaxies at $z \gtrsim 4$ and the Evolution of the Ultraviolet Luminosity Density at High Redshift *ApJ* **519**, 1–17.

Strateva, I., et al. 2001 Color Separation of Galaxy Types in the Sloan Digital Sky Survey Imaging Data *AJ* **122**, 1861–1874.

Toomre, A., & Toomre, J. 1972 Galactic Bridges and Tails *ApJ* **178**, 623–666.

Tully, R. B., Pierce, M. J., Huang, J. S., Saunders, W., Verheijen, M. A. W., & Witchalls, P. L. 1998 Global Extinction in Spiral Galaxies *AJ* **115**, 2264–2272.

van Kampen, E., Jimenez, R., & Peacock, J. A. 1999 Overmerging and mass-to-light ratios in phenomenological galaxy formation models *MNRAS* **310**, 43–56.

White, S. D. M., & Frenk, C. S. 1991 Galaxy formation through hierarchical clustering *ApJ* **379**, 52–79.

White, S. D. M., & Rees, M. J. 1978 Core condensation in heavy halos — A two-stage theory for galaxy formation and clustering *MNRAS* **183**, 341–358.

Witt, A. N., & Gordon, K. D. 2000 Multiple Scattering in Clumpy Media II. Galactic Environments *ApJ* **528**, 799–816.

Wolf, C., Meisenheimer, K., Rix, H.-W., Borch, A., Dye, S., & Kleinheinrich, M. 2003 The COMBO-17 survey: Evolution of the galaxy luminosity function from 25 000 galaxies with $0.2 < z < 1.2$ *A&A* **401**, 73–98.

Worthey, G. 1994 Comprehensive stellar population models and the disentanglement of age and metallicity effects *ApJS* **95**, 107–149.

Wyuts, S., van Dokkum, P. G., Kelson, D. D., Franx, M., Illingworth, G. D. 2004

The Detailed Fundamental Plane of Two High-Redshift Clusters: MS 2053-04 at $z = 0.58$ and MS 1054-03 at $z = 0.83$ *ApJ* **605**, 677–688.

Yan, L., & Thompson, D. 2003 Hubble Space Telescope WFPC2 Morphologies of K-selected Extremely Red Galaxies *ApJ* **586**, 765–779.

Yee, H. K. C., & Ellingson, E. 1995 Statistics of close galaxy pairs from a faint-galaxy redshift survey *ApJ* **445**, 37–45.

York, D. G., et al. 2000 The Sloan Digital Sky Survey: Technical Summary *AJ* **120**, 1579–1587.

Zepf, S. E., & Koo, D. C. 1989 Close pairs of galaxies in deep sky surveys *ApJ* **337**, 34–44.